J. Biochem. **136**, 377–386 (2004)
DOI: 10.1093/jb/mvh136

In Vitro and *In Vivo* Effects of the Overexpression of Osteopontin on Osteoblast Differentiation Using a Recombinant Adenoviral Vector

Hiroko Kojima[1,2], Toshimitsu Uede[3] and Toshimasa Uemura[1,2,4,*]

[1]Age Dimension Research Center, National Institute of Advanced Industrial Science and Technology (AIST), Tsukuba Central-6, Tsukuba 305-8566; [2]JST(Japan Science and Technology Agency); [3]Division of Molecular Immunology, Institute for Genetic Medicine, Hokkaido University, Sapporo; and [4]Department of Orthopedic Surgery, Tokyo Medical and Dental University, 1-5-45 Yushima, Bunkyo-ku, Tokyo 113-8519

Received May 20, 2004; accepted June 24, 2004

Osteopontin (OPN) is a highly acidic secreted phosphoprotein that binds to cells via an RGD (arginine-glycine-aspartic acid) cell adhesion sequence that recognizes the $\alpha_V\beta_3$ integrin. OPN may regulate the formation and remodeling of bone. To elucidate the function of OPN in bone tissue, we examined the overexpression of OPN in osteoblasts *in vitro* and *in vivo* using an adenoviral vector carrying an OPN cDNA (Adv-OPN). Rat bone marrow–derived osteoblasts infected with Adv-OPN were examined by Western blotting, immunofluorescence, nodule formation measurements, assay of alkaline phosphatase (ALP) activity, and Northern blotting. The results suggested that not only osteoblast differentiation markers such as osteocalcin and ALP, but nodule formation and ALP activity are markedly enhanced by OPN overexpression in the case of viral infection. On the contrary, when Adv-OPN and uninfected osteoblasts were implanted into subcutaneous sites with a porous ceramic scaffold, the ALP activity and calcium content of the OPN-infected composite were higher than in uninfected composites, however, the differences were smaller than expected from the *in vitro* experiments. We speculate that the difference in the result of *in vitro* and *in vivo* experiments originates from the inhibitory effect of secreted OPN on the crystal growth of apatite *in vivo*, which competes with the induced activity of osteoblasts.

Key words: adenovirus, osteoblast, osteopontin, overexpression.

Osteopontin (OPN) is a highly acidic secreted phosphoprotein that binds to cells via an RGD (arginine-glycine-aspartic acid) cell adhesion sequence that recognizes the $\alpha_V\beta_3$ integrin. Numerous functions have been ascribed to OPN. OPN exhibits a restricted distribution in healthy adult humans and animals. The highest levels are found in bone and kidney, and most epithelial lining cells in the body express OPN. OPN is also found in most body secretions including urine, saliva, milk and bile (*1*). The functions of OPN in kidney have been reported to include the regulation of renal iNOS and urinary calcium oxalate deposition (*2*). In contrast to the limited distribution in healthy tissue, OPN expression in disease and injury has been shown to be markedly upregulated under conditions of inflammation and tissue remodeling (*3*). In addition, OPN expression is induced in multiple cell types, including macrophages and angiogenic endothelial cells, during the granulation phase of wound healing in soft and hard tissues (*4*). In angiogenic endothelial cells, OPN promotes endothelial migration and survival during new capillary formation through interaction with $\alpha_V\beta_3$ integrin (*5*, *6*).

OPN may regulate the formation and remodeling of mineralized tissues (*7*, *8*) in bone. Generally, three different functions of osteopontin in bone have been proposed based on *in vitro* and *in vivo* findings (3): 1) regulation of bone cell adhesion, 2) regulation of osteoclast function, and 3) regulation of matrix mineralization. OPN is considered to promote the attachment of osteoblasts, allowing them to perform the functions necessary for osteogenesis (*9*). We have reported the inducible function of OPN in the differentiation of primary osteoblasts (*10*). Our study also indicated that the binding of OPN to integrin $\alpha_V\beta_3$ regulates intracellular signal transduction to upregulate ALP and OCN expression via FAK (focal adhesion kinase) phosphorylation in osteoblasts (*11*). A developmental study using rat embryonic tissues indicated that OPN is synthesized and secreted by bone cells in the early stages of the osteogenesis of several osseous tissues and in the synthesis of osteocalcin (*12*). In this role, OPN is likely to assist in bone formation. However, there has been no published report directly indicating the effect of OPN on nodule formation by osteoblasts. We have examined the effect of OPN overexpression on nodule formation in osteoblasts. Many studies have focused on the role of osteopontin in osteoclast function, suggesting that the OPN is an important regulator of osteoclasts via interactions with $\alpha_V\beta_3$ integrin (*13–20*). OPN mediates initial osteoclast recognition and attachment to bone through $\alpha_V\beta_3$ integrin. Secondly, OPN regulates osteoclast functions, including bone resorption. Furthermore, OPN is a potent inhibitor of both *de novo* apatite formation and apatite growth, as a result of OPN binding to apatite surfaces. The phosphorylation might play a regulatory role in controlling apatite crystal growth (*21–23*). As described above, OPN has multiple functions in mineral-

*To whom correspondence should be addressed. Tel: +81-29-861-2724, Fax: +81-29-861-2789, E-mail: t.uemura@aist.go.jp

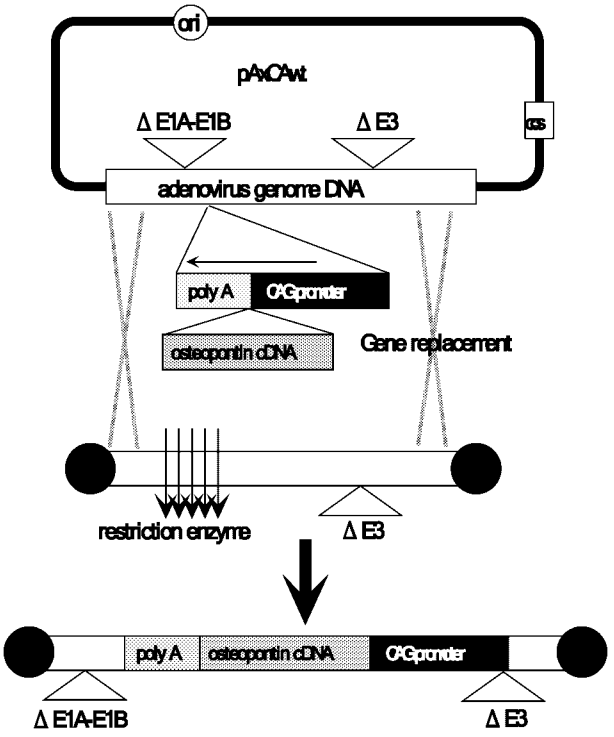

Fig. 1. **Generation of a recombinant adenoviral vector carrying the OPN gene (Adv-OPN).**

ization via the contributions of osteoblasts and osteoclasts, but also in the growth of hydroxyapatite.

Several systematic studies have been conducted using $OPN^{-/-}$ mice in order to understand the role of OPN *in vivo*. OPN null mice show no abnormalities in either bone or tooth development, in comparison with their skeletal size and patterning (*23*). The study suggests that other kinds of matrix molecules might contribute to bone remodeling during embryonic development. The amount of Ca released from OPN-deficient bones does not differ significantly from that released from wild type bones; however, parathyroid hormone (PTH)–induced bone resorption does not occur in OPN-deficient bones (*24*). Moreover, the enhancement of osteoclastic bone resorption and suppression of osteoblastic bone formation in response to reduced mechanical stress do not occur in OPN-deficient bones (*25*). These results suggest that OPN plays a very important role in bone remodeling; however, the real function of OPN remains unclear. One reason for the uncertainty is that the above mentioned three functions of OPN may simultaneously contribute to bone remodeling in a complex manner *in vivo*. From this point of view, we designed the present experiment to simplify the complexity *in vivo*. First, to clarify the role of OPN in bone more directly, we constructed an adenoviral vector carrying an OPN cDNA (Fig. 1) and examined the overexpression of OPN in rat bone marrow–derived osteoblastic primary cells *in vitro*. Second, the OPN-overexpressing osteoblasts were transplanted into ectopic (subcutaneous) sites to exclude the effect of osteoclasts appearing in orthotopic sites. The results in OPN-overexpressing osteoblasts *in vitro* and after transplantion into subcutaneous sites in rats are discussed.

MATERIALS AND METHODS

Cells and Culture—Experiments were performed in accordance with the guidelines of the Japanese Government for the care and use of laboratory animals. Rat bone marrow-derived osteoblastic primary cells were obtained from Fischer 344 male rats (7-wk-old) according to the method of Maniatopoulos *et al.* (*26*). For primary culture, the femora were removed and washed with MEM (Nacalai Tesque, Kyoto, Japan) containing 15% fetal bovine serum (FBS) (Sigma, St Louis, MO, USA) and antibiotic-antimycotic (Invitrogen Corp., Carlsbad, CA, USA). The epiphyses of bone sides were removed and the marrow cavity was flushed out with the above medium using a syringe with a 21-gauge needle. The osteoblastic primary cells were cultured in T-75 culture flasks (BD Falcon, Bedford, MA, USA) at 37°C in a humidified atmosphere of 95% air with 5% CO_2 for 10 d until nearly confluent. Subsequently, cells were treated with 0.1% trypsin including 0.02% EDTA, and subcultured under the appropriate conditions for the following experiments.

Construction of a Recombinant Adenoviral Vector Carrying the OPN Gene—The plasmid carrying the OPN cDNA was kindly provided by Dr. M. Inobe (Hokkaido Univ.). The OPN cDNA was obtained by digestion of the plasmid with *Xba*I and *Sac*I. Recombinant adenoviral vectors carrying an expression cassette containing the cytomegalovirus IE enhancer, chicken β-actin promoter, mouse OPN cDNA, and the rabbit β-globin poly (A) signal were constructed using an Adenovirus Expression Vector Kit (TaKaRa, Shiga, Japan). The end of the cDNA was blunted for subcloning into the SwaI site of the pAxCAwt cosmid. The cosmid and adenoviral DNA-terminal protein complex were co-transfected into the E1-transcomplemental cell line 293. The recombinant adenoviruses (Adv-OPN) generated by homologous recombination were isolated, and the insertion was confirmed by digestion with restriction enzymes. An adenoviral vector without the OPN insert (Adv-mock) was used as another control (mock).

Western Blotting—Cells were seeded at 3×10^5 cells/well on ϕ 3.5 cm dishes in MEM containing 15% FBS, antibiotic-antimycotic, and an osteoblastic supplement (10 mM β-glycerophosphate [Sigma], 50 μg/ml of L-ascorbic acid phosphate [Wako, Osaka, Japan], and 10 nM dexamethasone [Sigma]). The next day (day 0), the cells were infected with Adv-OPN at an appropriate multiplicity of infection (moi) or Adv-mock (moi = 50) in 100 μl of MEM containing 5% FBS for 1 h. On the days indicated after infection, total proteins were extracted with 2× SDS sample buffer and heated at 95°C for 5 min. The proteins were separated in 10% SDS-polyacrylamide gels, transferred to a polyvinylidene difluoride filter, and probed with a mouse monoclonal anti-rat osteopontin (MPIIIB10 (1), DHSB, Univ. Iowa) antibody. Western blot analysis was performed according to the method recommended in the company protocol using the BCIP/NBT Phosphatase Substrate System (KPL, Gaithersburg, MD, USA).

ELISA—OPN secreted into the culture medium was quantitated using a mouse osteopontin EIA kit (Immuno-Biological Laboratories Co., Ltd., Gunma Japan) according to the manufacturer's instructions. The ELISA kit is designed to detect mouse and rat OPN with a detection

limit 1 μg/ml, and 4–5% intra-assay, and 10–16% inter-assay variability.

Immunofluorescence Staining—Cells were plated on coverslips, and infected the next day with Adv-OPN at a moi of 10 and 50 or Adv-mock at a moi of 50. Uninfected cells were also used as another control. One, 3 and 7 d after infection, cells were washed with PBS and fixed with 4% paraformaldehyde/PBS for 10 min. The fixed cells were washed with PBS and incubated in PBS containing 2% skim milk for 2 h at room temperature. The anti-rat osteopontin (MPIIIB10) antibody was diluted in PBS containing 3% bovine serum albumin (BSA) placed as a drop on the coverslips, and incubated overnight at 4°C. The coverslips were washed with PBS and incubated with a FITC-conjugated goat anti-mouse IgG (Wako) in PBS for 2 h at 37°C. The cells were also stained with DAPI (nuclei) and phalloidine-rhodamin (actin) according to the laboratory protocol. The coverslips were then washed with PBS and were mounted with glycerin containing PPD and observed under a microscope (Olympus IX-70, Tokyo Japan).

Northern Blotting—Cells were seeded at 3×10^5 cells/well on ϕ 3.5 cm dishes in MEM containing 15% FBS, antibiotic-antimycotic, and an osteoblastic supplement. Twenty-four hours later (day 0), the cells were exposed to Adv-OPN at a moi of 10 or 50 or Adv-mock at a moi of 50 in 100 μl of MEM containing 5% FBS for 1 h. Uninfected cells were also used as another control. Then, 3 ml of culture medium was added to dilute the viruses. On the days indicated after infection, total RNA was isolated from the osteoblast cells using TRIzol (Gibco) according to the manufacturer's instructions. Aliquots (20 μg) of total RNA were separated in a 1% agarose/5.5% formaldehyde gel and blotted onto a Hybond™-XL membrane (Amersham Pharmacia Biotech, Buckinghamshire, UK). Probes for cDNA encoding rat OPN, rat alkaline phosphatase (ALP) and rat osteocalcin (OCN) were labeled with α-^{32}P dCTP (3000 Ci/mmol, Amersham Pharmacia Biotech) using rediprime™ (Amersham Pharmacia Biotech). After hybridization at 68°C for 3 hours in PerfectHyb™ Plus HYBRIDIZATION BUFFER (Sigma) with the labeled cDNA probe (2×10^6 cpm/ml), the membrane was washed with 2× SSC/0.1% SDS, and then twice with 0.5× SSC/0.1% SDS. The washed blot was exposed and quantitated with Image Quant software (Amersham Bioscience). The ratio of the signal intensity to that of 28S was calculated.

Alkaline Phosphatase (ALP) Activity—Cells were seeded at 3×10^5 cells/well on ϕ 3.5 cm dishes (three dishes for each group) and infected the next day with Adv-OPN at a moi of 10 or 50 or Adv-mock at a moi of 50. Uninfected cells were also used as another control. On the days indicated after infection, cells were harvested by low speed centrifugation, and disrupted in 0.1 M Tris-HCl (pH 7.4) containing 1% Triton X-100 and 5mM $MgCl_2$ by sonication. After centrifugation at $6{,}000 \times g$ for 10 min, the supernatants were collected. Aliquots of 2.5 μl from each sample were added to 250 μl of alkaline phosphatase substrate buffer containing 0.056 M 2-amino-2-methyl-1,3-propandiol (pH9.0), 10 mM *p*-nitrophenyl phosphate, and 2mM $MgCl_2$, and the samples were incubated at 37°C for 30 min. The enzymatic activity of alkaline phosphatase was calculated after measuring the absorbance of the *p*-nitrophenol product at 405 nm on a microplate reader (Bio-Rad, Hercules, CA, USA). The activity was expressed as mM of *p*-nitrophenol.

Calcium Content—Seven, 14, and 21 d after infection, Adv-OPN–infected (moi 10 or 50), Adv-mock–infected (moi = 50) and uninfected (control) osteoblastic primary cells were fixed with 10% formalin–neutralized buffer for 15 min and extracted with 0.6 M HCl at 4°C overnight. The calcium content of each sample was determined with a calcium assay kit (Cat. 587, Sigma) according to the manufacturer's instructions.

Alizarin Red Staining—Cells were fixed with 10% formalin–neutralized buffer for 15 min, stained with 1% alizarin red (pH 4.0) for 2 min, and then washed with deionized water.

Nodule Formation Assay—Cells were seeded at 3×10^5 cells/well on ϕ 3.5 cm dishes and infected the next day with Adv-OPN at a moi of 50. Seven days after infection, the cells were fixed with 10% formalin–neutralized buffer for 15 min, and stained by the von Kossa staining method to evaluate bone nodule formation. The microscopic images of von Kossa stained cells were analyzed using MetaMorph software to evaluate total nodule formation ($n = 2$).

Cultured Bone Tissue Implantation Model—β-Tricalcium phosphate (β-TCP) cubic porous blocks ($5 \times 5 \times 5$ mm3) were kindly provided by Olympus Optical, Co. Ltd. (Tokyo, Japan) (*27*). The solid and porous component of the microstructure is well interconnected. The average pore size is 200 μm in diameter. The procedures of the transplantation (*28*) were as follows. After 10 d of primary culture, cells were treated with 0.25% trypsin and 0.02% EDTA, harvested by low speed centrifugation, and resuspended in fresh medium at a concentration of 2×10^6 cells/ml. β-TCP blocks were soaked in the cell suspension under low pressure (150 mmHg) for 1 min, and then incubated for 2 h in a CO_2 incubator. The blocks were transferred to 24-well plates (single block per well) and cultured in 2 ml of MEM with 15% FBS, antibiotic-antimycotic, and the osteoblastic supplement for 2 wk. The cells/β-TCP composites were incubated in MEM with 5% FBS containing Adv-OPN (6.2×10^8 plaque forming units [pfu]/ml) for 2 h. Then the composites were added to MEM containing 15% FBS, antibiotic-antimycotic, and the osteoblastic supplement, and cultured for 24 h. Untreated cell/β-TCP composites were used as a control. These composites were implanted subcutaneously in the backs of Fischer rats; three treated composites were implanted separately on the right side, and control composites were implanted separately on the left side.

Biochemical Analysis of Implanted Blocks—The composites were harvested and subjected to biochemical analysis at 2 and 4 wk after implantation. The composites were homogenized in 0.5 ml of 0.1 M Tris (pH 7.4) containing 1% Triton X-100 and 5 mM $MgCl_2$, and centrifuged at $6{,}000 \times g$ for 10 min at 4°C. The supernatant was assayed for alkaline phosphatase activity as described above. Calcium was extracted from the sediment with 5 ml of 20% formic acid over a period of 1 wk at 4°C. The calcium content of each sample was determined with a calcium assay kit (Cat. 587, Sigma) according to the manufacturer's instructions.

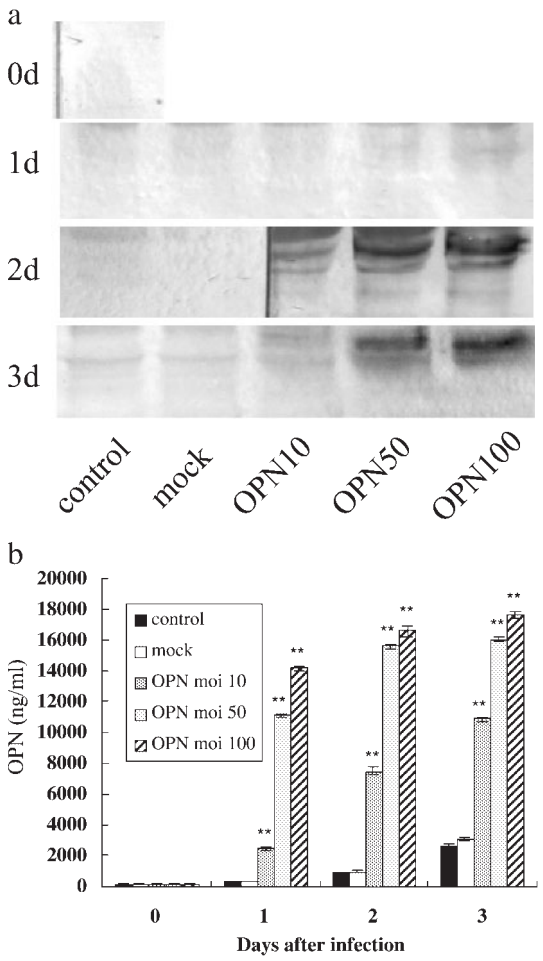

Fig. 2. **(a) Time course and moi dependence of the Western blotting pattern of OPN expressed in Adv-OPN–infected (moi = 10, 50 and 100), Adv-mock–infected (mock) and uninfected (control) primary osteoblastic cells.** Each experiment was performed twice independently (n = 2). **(b) Time course and moi dependence of the amount of OPN secreted from Adv-OPN–infected (moi = 10,50 and 100), Adv-mock–infected (mock) and uninfected (control) primary osteoblastic cells into the culture medium.** Each experiment was performed twice independently (n = 2).

Statistical Analysis—Average values of OPN content, ALP activity, calcium content, nodule formation were calculated, expressed as the arithmetic means ± SE, and plotted. The data were analyzed by paired t test. Paired t test was used for statistical evaluation. The statistical significance was established at the $^{*}p < 0.05$ and $^{**}p < 0.01$ level.

SEM Observation—The β-TCP/osteoblasts composites were evenly cut in the center for use as SEM samples. Then samples were fixed with 2% paraformaldehyde/2.5% glutaraldehyde in 0.1 M cacodylate buffer (pH 7.4), postfixed with 0.1% osmium tetroxide (OsO_4), dehydrated in a graded series of alcohol solutions, and dried in a critical point dryer. The samples were glued onto stubs with tape, sputter-coated with platinum in an ion coater (Meiwa, PMC-5000, Tokyo, Japan), and observed by SEM (Hitachi, S-4500, Japan).

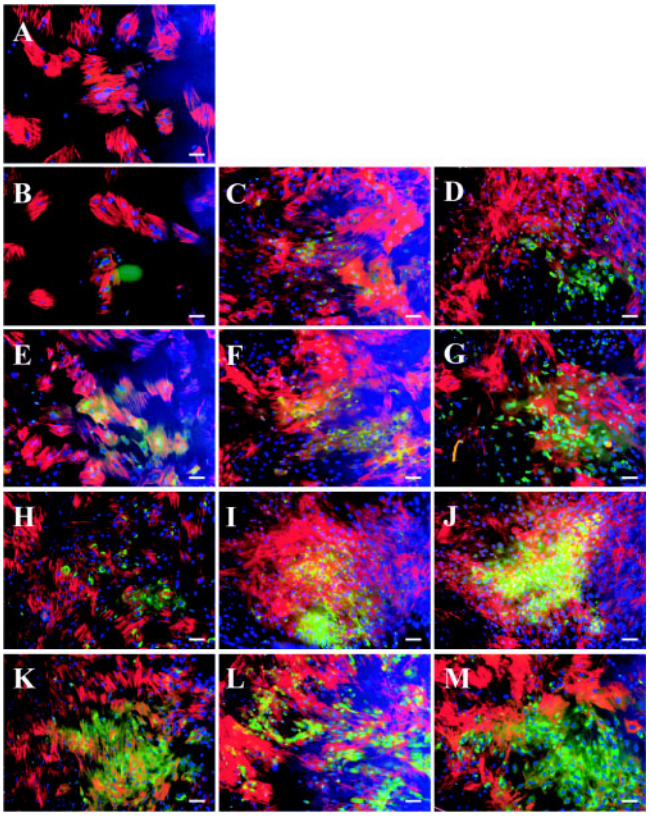

Fig. 3. **Immunofluorescence staining of osteopontin on uninfected (control) (B, C, D), Adv-mock–infected (E, F, G), and Adv-OPN–infected (moi = 10 [H, I, J] and moi=50 [K, L, M]) on day 1 (B, E, H, K), day 3 (C, F, I, L) and day 7 (D, G, J, M) after infection.** A shows the data at day 0. Cells were stained with DAPI (nuclei: blue), anti-OPN antibody (OPN:green) and rhodamine-phalloidin (actin: red). Bar = 100 μm. Each experiment was performed twice independently (n = 2).

RESULTS

In Vitro Effect of OPN Overexpression in Primary Osteoblasts—Expression of the OPN protein in Adv-OPN–infected primary osteoblasts: To examine the effect of OPN overexpression on the differentiation of osteoblasts *in vitro*, we used rat bone marrow–derived primary osteoblasts, cultured by the method of Maniatopoulos *et al.*, which were infected with Adv-OPN or Adv-mock (adeno viral control without OPN insert), or uninfected (control). Figure 2a shows the moi dependence of the western blotting pattern of OPN expressed in Adv-OPN infected primary osteoblasts on days 0, 1, 2 and 3 after infection. On day 1, little OPN signal was detected under any conditions, indicating that this is the intrinsic expression of OPN in primary osteoblasts. On days 2 and 3, a clear and strong Western blot pattern was detected and this increased as the moi increased, confirming that the Adv-OPN works in the primary osteoblasts. Figure 2b shows the time course and moi dependence of the amount of OPN secreted into the medium. As the moi increased, the amount of OPN increased, appearing saturated at moi 50 and 100. The time course shows a steady increase until day 3. The amount of OPN secreted from control/(unin-

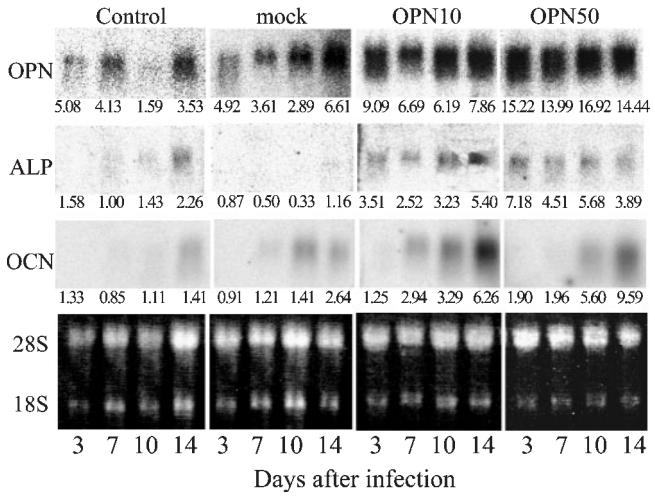

Fig. 4. **Effect of OPN overexpression on the expression of osteoblast markers, alkaline phosphatase (ALP) and osteocalcin (OCN) at the transcriptional level.** Northern blot analysis of Adv-OPN–infected (moi = 10, 50), Adv-mock–infected (moi = 50) and uninfected (control) osteoblastic primary cells was performed on 3, 7, 10, 14 d after infection. The values under the signals are the ratios of signal intensity to that of 28S. Each experiment was performed twice independently (n = 2).

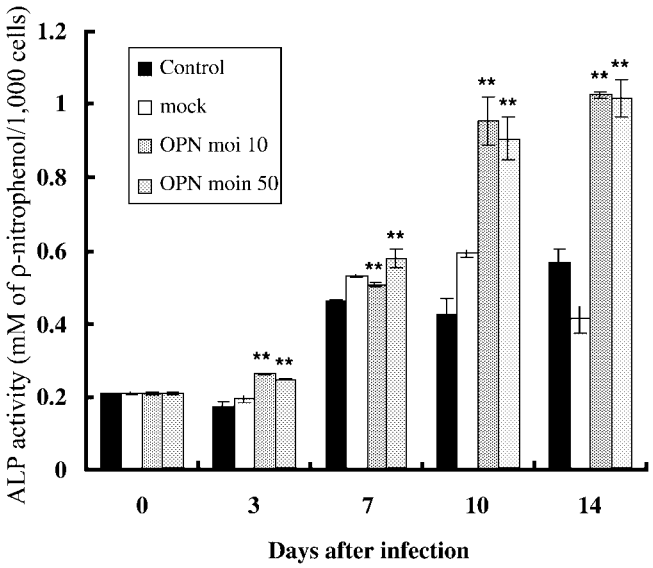

Fig. 5. **Alkaline phosphatase activity of Adv-OPN–infected (moi=10,50), uninfected (control) and Adv-mock–infected (moi = 50) osteoblastic primary cells on 0, 3, 7, 10 and 14 d after infection.** Each experiment was performed 4 times independently (n = 3).

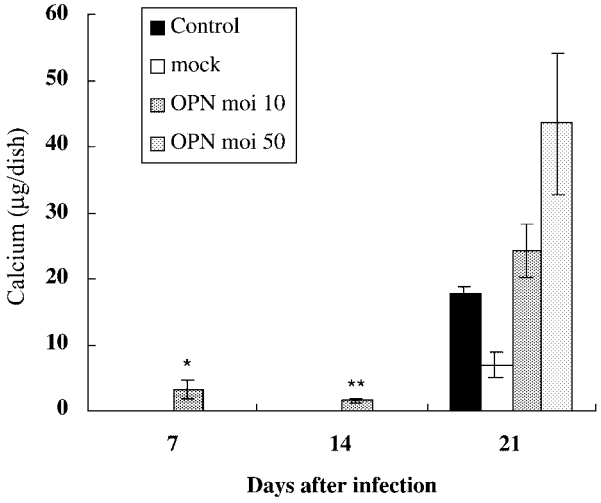

Fig. 6. **Calcium content of Adv-OPN-infected (moi = 10, 50), uninfected (control) and Adv-mock infected (moi = 50) osteoblastic primary cells on 7, 14 and 21 d after infection.** Each experiment was performed 4 times independently (n = 3).

fected) and Adv-mock–infected cells showed similar patterns, and the amount was much smaller than that in Adv-OPN–infected cells. The signals for the two control cells is believed to arise from intrinsic OPN expression in osteoblasts.

Immunofluorescence images of OPN in Adv-OPN-infected osteoblasts on days 1, 3 and 7 after infection are shown in Fig. 3. Weak signals were detected in the two control groups (B–D, E–G), suggesting weak intrinsic OPN expression; however, a strong fluorescence signal for FITC (green) was detected in the Adv-OPN-infected group (H–J, K–M) with the strongest signal on day 7 (M) at moi = 50.

Bone forming activity of Adv-OPN–infected primary osteoblasts: Figure 4 shows the Northern blot analysis of OPN and two typical osteogenic markers (alkaline phosphatase (ALP) and osteocalcin (OCN)) in Adv-OPN–infected (moi = 10, 50), Adv-mock–infected (moi = 50) and uninfected (control) primary osteoblasts. The ratios of the signal intensities to those of 28S are shown beneath each Northern signal. The results indicate that OPN expression at the transcriptional level was strong, even on day 3 and the level remained high until day 14. The strongest expression was detected at moi = 50. In contrast, expression of osteocalcin (OCN) showed a steady increase until day 14. The expression of alkaline phosphatase showed little time dependence. The ALP activities of Adv-OPN–infected cells and control cells showed different time dependencies from expression at the transcriptional level, as shown in Fig. 5. Until day 7, the ALP activities of Adv-OPN–infected (moi = 10,50), Adv-mock–infected (moi = 50) and uninfected (control) osteoblasts showed similar levels and time courses, suggesting that the ALP activity until day 7 comes from intrinsic activity without any effect of virus infection. On day 10, the ALP activities of Adv-OPN–infected cells (moi = 10, 50) differed from those of Adv-mock–infected and uninfected cells. At day 14, a marked enhancement was detected, suggesting the effect of OPN overexpression.

The calcium content (Fig. 6) shows a remarkable effect of OPN overexpression on day 21 (moi = 50) despite a negligible effect until day 14.

Figure 7 shows the results of Alizarin red staining and nodule formation in Adv-OPN–infected, Adv-mock–infected and uninfected osteoblasts. We detected the moi dependence of nodule formation in Adv-OPN-infected cells and found no difference between the two controls (uninfected and Adv-mock-infected), which both showed little nodule formation. To clarify the effect of OPN over-

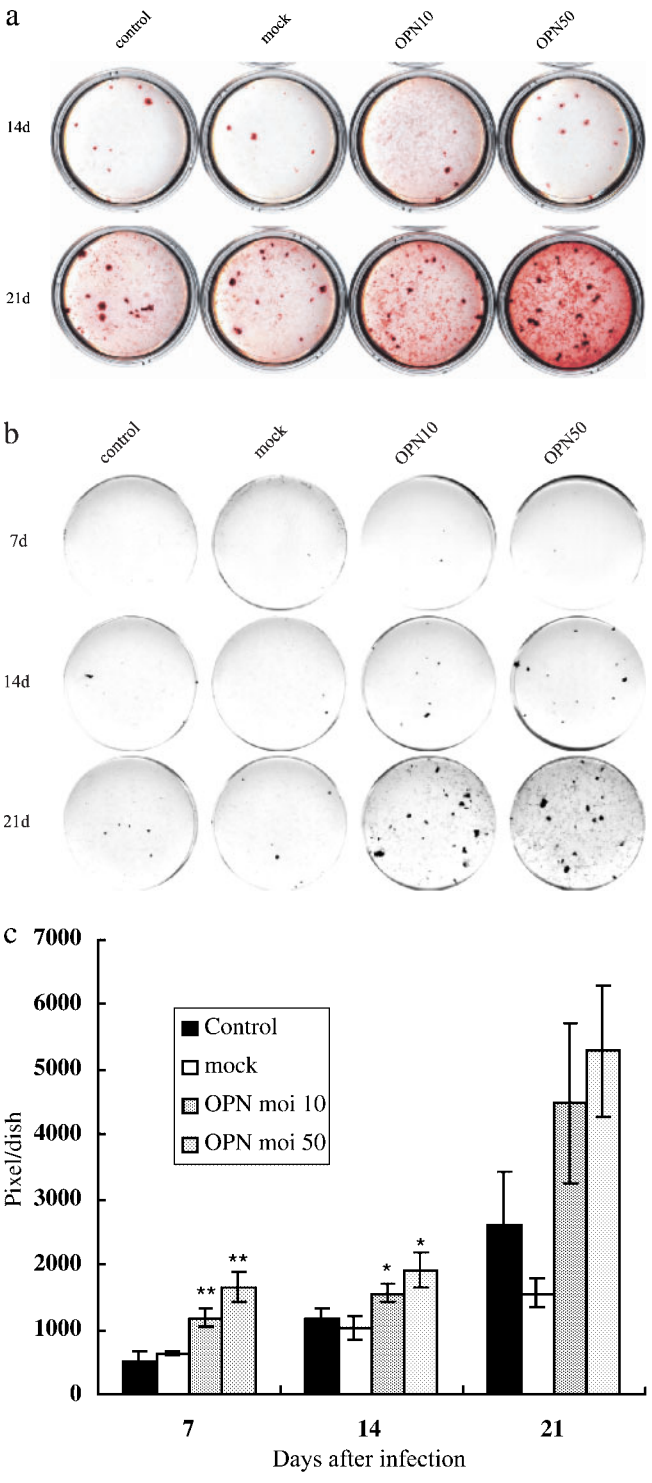

Fig. 7. **(a) Alizarin red staining of Adv-OPN–infected (moi = 10, 50), uninfected (control) and Adv-mock–infected (moi = 50) primary osteoblastic cells 14 and 21 d after infection.** Each experiment was performed twice independently (n = 2). **(b) Von Kossa staining of Adv-OPN–infected (moi = 10, 50), uninfected(control) and Adv-mock–infected (moi = 50) osteoblastic primary cells 7, 14 and 21 d after infection.** Each experiment was performed twice independently (n = 2). **(c) Numerical analysis of the images of the von Kossa stained osteoblastic primary cells shown in (b).** The integrated values of the intensity at each pixel in the stained area were plotted. Each experiment was performed twice independently (n = 2).

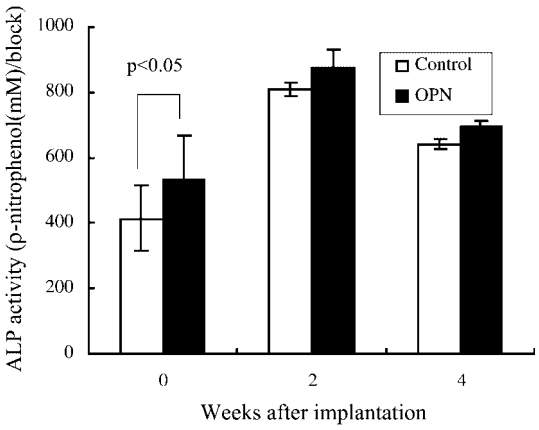

Fig. 8. **Alkaline phosphatase activity of implanted osteoblastic primary cells (Adv-OPN–infected and uninfected) at 0, 2, and 4 wk after implantation.** Each experiment was performed twice independently (n = 6).

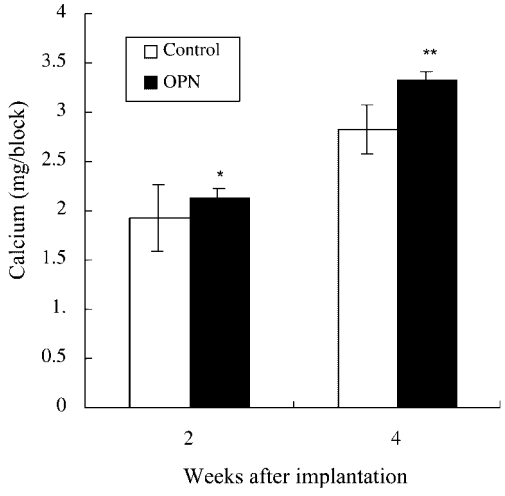

Fig. 9. **Calcium contents of implanted osteoblastic primary cell/porous ceramic blocks (Adv-OPN–infected and uninfected) 2 and 4 wk after implantation.** Each experiment was performed twice independently (n = 6). $^{*}p < 0.05$ *vs.* control; $^{**}p < 0.001$ *vs.* control)

expression on nodule formation, the microscopic images of von Kossa stained cells were numerically analyzed using MetaMorph software (Molecular Devices). The results shown in Fig. 7c indicate a clear effect of OPN overexpression on nodule formation at moi = 50. The time course of nodule formation shows a remarkable enhancement on day 21 in the case of OPN overexpression, despite the small enhancement until day 14. Adv-OPN infected cells (moi = 50) formed at least twice as many nodules as control cells.

In Vivo Effect of Osteopontin Overexpression on Implanted Primary Osteoblasts—We examined the effects of osteopontin overexpression on primary osteoblast/porous ceramic composites implanted subcutaneously into Fischer rats. *In vitro* experiments using Adv-mock–infected cells and uninfected cells showed no marked difference between the two. Moreover, it is difficult to exam-

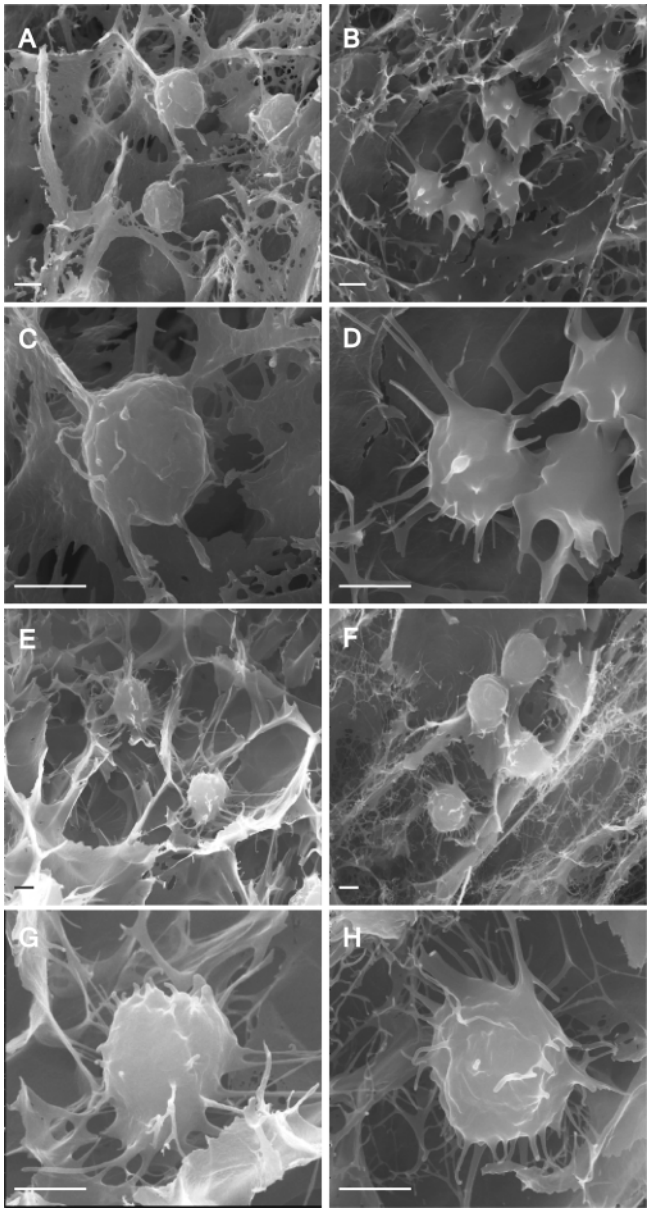

Fig. 10. **SEM images of implanted osteoblastic primary cells (Adv-OPN–infected [B, D, F, H] and uninfected [A, C, E, G]), 2 (A, B, C, D) and 4 (E, F, G, H) wk after implantation at low (A, B, E, F) and high (C, D, G, H) magnifications.** Each experiment was performed twice independently (n = 2). Bar = 10 μm.

ine many samples in *in vivo* experiments. We omitted Adv-mock–infected cells in the *in vivo* study.

Figure 8 shows the ALP activity of infected and uninfected cell/porous ceramic composites at 0, 2 and 4 wk postimplantation. The overexpression of osteopontin produced a slight increase in ALP activity after infection; however, the large induction expected from the *in vitro* experimental data was not achieved. The calcium contents of the infected and uninfected primary osteoblast/porous ceramic composites are shown in Fig. 9. The effect of osteopontin overexpression was 10% and 18% at 2 and 4 wk postimplantation.

Figure 10 shows SEM images of implanted cells in the porous ceramic composites 2 (A, B, C, D) and 4 (E, F, G, H) wk postimplantation. In spite of the unexpectedly small effect on ALP activity and calcium content, the infected cells showed different morphological features than control cells at 2 weeks postimplantation. Control cells appeared round (A, C), while the infected cells had many processes on their surface, and their shape was more spread out (B, D). Many infected and control cells showed similar features (data not shown). At 4 wk postimplantation, the difference was not as clear as at two weeks. Morphological observations indicated that the collagen production might be enhanced by OPN overexpression.

DISCUSSION

Bone matrix proteins such as collagen type I, OPN, BSP, osteonectin, and osteocalcin have been investigated by many researchers. Among them, OPN is a typical noncollagenous bone protein and the bone is the organ that shows the highest OPN content. To study the role of OPN in osteoblasts, some researchers have focused on the effects of OPN when used as a matrix for cell attachment (*11*, *29–30*). OPN has been reported to affect osteoblast adhesion and signal transduction pathways by inducing FAK phosphorylation, MAPK activation and cytokine activation of osteoblasts. However, nodule formation activity has not been reported. Moreover, in spite of our general concept that OPN binds to integrin $\alpha_V\beta_3$, some researchers showed negative binding results (*31*, *32*), suggesting another integrin might be important in OPN binding. Thus OPN overexpression in osteoblasts *in vitro* might be a short way to elucidate the function of OPN in osteoblasts. It is true that our expression system induced a much higher level of OPN expression than the endogeneous level. However, to elucidate the function of OPN, osteoblasts that express OPN endogeneously should be used. To elucidate the function of OPN in a system including OPN, an OPN expression system producing a high level of OPN should be used. Otherwise the effect of OPN overexpression can not be detected. To study the physiological function of OPN, we used osteoblasts expressing OPN at a physiological level and studied the effect of OPN overexpression.

For the further study of OPN function in osteoblasts *in vivo*, we chose ectopic (subcutaneous) sites for the implantation of OPN overexpressing osteoblasts for the following reasons. As described in the introduction, three different functions of osteopontin in bone have been proposed based on *in vitro* and *in vivo* findings (3): 1) regulation of bone cell adhesion; 2) regulation of osteoclast function; and 3) regulation of matrix mineralization. Of these three functions, the second one makes our understanding of the *in vivo* function of OPN more difficult, because osteoclasts activated by OPN have functions opposite to those of osteoblasts (function (a)) and are expected to disturb the inhibition function of mineralization by resorbing apatite. From this point of view, we chose an experimental model system that excludes the effect of osteoclasts *in vivo*. An experimental *in vivo* model that satisfies the above requirement is osteoblasts that overexpress OPN *in vitro* and are then implanted into ectopic (subcutaneous) sites where no osteoclasts appear. Furthermore, because there is no bone in the subcutaneous site, new bone formation is easily observed and detected.

Biochemical assays, such as for ALP activity or Northern blotting, can easily be performed.

OPN is considered to promote the attachment of osteoblasts, allowing them to perform the functions necessary for osteogenesis (*7*, *8*). Our previous study indicated that the binding of OPN to integrin $\alpha_V\beta_3$ regulates intracellular signal transduction to upregulate ALP and OCN expression via FAK (focal adhesion kinase) phosphorylation in osteoblasts (*11*). A developmental study using rat embryonic tissues indicated that OPN is synthesized and secreted by bone cells in the early stage of osteogenesis of several osseous tissues and the synthesis of osteocalcin (*12*). In this case, OPN is likely to form bone. However, there have been no reports directly indicating the effect of OPN on nodule formation by osteoblasts. Our study clealy demonstrates that the overexpression of OPN induces nodule formation in osteoblasts, as shown in Fig. 7. However, the *in vivo* experimental data did not show a marked enhancement in bone formation despite the data obtained *in vitro*.

The *in vitro* data support a positive effect of OPN overexpression on osteoblast differentiation and activity. First, we confirmed that Adv-OPN worked well in the primary osteoblasts by Western blot analysis (Fig. 2) and immunofluorescence staining (Fig. 3) of the expressed OPN protein. Second, we demonstrated the effect of OPN overexpression by Northern blot analysis of osteogenic markers (Fig. 4), alkaline phosphatase activity (Fig. 5), calcium content (Fig. 6) and nodule formation (Fig. 7) in Adv-OPN–infected, Adv-mock–infected and uninfected (control) osteoblasts. The *in vitro* data obtained in these experiments strongly support an inducible effect of OPN overexpression on osteoblast differentiation and activity.

Based on these *in vitro* results, the overexpression of OPN may lead to gene therapy in orthopedic fields such as BMP (bone morphogenetic protein) gene therapy (*33*–*37*). However, the *in vivo* results are not so encouraging. At two weeks postimplantation, the alkaline phosphatase activity of implanted infected osteoblastic primary cells was 8% greater than that of control cells. Moreover, the calcium content in the culture of infected osteoblastic cells *in vivo* was 10 % more than that of control cells. These results demonstrate that the overexpression of OPN in osteoblasts has a small effect on bone formation ability of osteoblasts. To explain the contradictory results obtained *in vitro* and *in vivo*, we performed a morphological study of the implanted osteoblasts by scanning electron microscopy as shown in Fig. 10. Results showed that the infected cells had different morphological features from the control cells, suggesting that the infected cells were more differentiated. Therefore, OPN-infected osteoblasts might have the potential to form bone nodules, but this may be inhibited *in vivo* by certain factors. These results suggest that infection with Adv-OPN activates preosteoblasts and/or surrounding cells via the binding of integrin $\alpha_V\beta_3$ and secreted OPN. We speculate that the inhibition of bone formation activity was caused by the adhesion of secreted OPN to apatite, which inhibited or slowed the crystal growth of apatite formed by osteoblasts. The inhibitory effect of OPN on apatite crystal growth has been reported by Boskey *et al.* (*21*), and Hunter *et al.* (*22*). They reported that the inhibitory effect of OPN is dose-dependent and is abolished when phosphate groups are removed from OPN. Moreover, the properties of OPN knockout also demonstrate OPN can inhibit mineralization. Our speculations are supported by these positive and negative properties of OPN in bone formation.

As seen in Fig. 7a and b again, nodule formation was clearly induced by OPN overexpression *in vitro* despite the comparatively small effect on ALP activity. Furthermore, a small induction of nodule formation by OPN overexpression was detected *in vivo*. This is the major point of emphasis of this study. We observed a clear induction of nodule formation by OPN overexpression *in vitro*, however; we observed a small induction effect on nodule formation by OPN overexpression *in vivo*. Even in our simplified model, the difference between the *in vitro* and *in vivo* results is complex; however, we can explain the difference by the inhibitory effect of OPN on hydroxyapatite formation.

Our *in vivo* experiments were performed at subcutaneous sites where few host bone cells exist, including osteoblasts and osteoclasts. OPN is known to be present at osteoclast attachment sites and might play an important role in osteoclast differentiation and function (*10*, *38*, *39*. Our study was limited to a simplified model that excluded the contribution of osteoclasts via OPN. We expect osteoclasts to have a positive effect on the OPN overexpression system, because they may attach to the secreted OPN on the apatite surface and resorb hydroxyapatite, inducing crystal growth again, and the binding of OPN to newly formed hydroxyapatite is the same as binding to the β-TCP implants. To include the contribution of osteoclasts, a more sensitive experimental system is necessary, and is currently be planned in our laboratory.

In conclusion, to elucidate the function of OPN in bone tissue, we examined the overexpression of OPN in osteoblasts *in vitro* and *in vivo* using an adenoviral vector carrying the OPN cDNA (Adv-OPN). Rat bone marrow–derived osteoblasts infected with Adv-OPN were examined by Western blotting, immunofluorescence, nodule formation measurements, alkaline phosphatase (ALP) activity assay, and Northern blotting. The results suggest that not only osteoblast differentiation markers such as osteocalcin and ALP, but nodule formation and ALP activity, are markedly enhanced by OPN overexpression via the viral infection. In contrast, when Adv-OPN and uninfected osteoblasts were implanted into subcutaneous sites with a porous ceramic scaffold, the ALP activity and calcium contents of the OPN-infected composites were higher than those of uninfected composite. However, the differences were smaller than expected from the *in vitro* experiments. The implanted infected cells appeared as active osteoblasts with bone formation activity in SEM analysis. We speculate that the differences between the results of the *in vitro* and *in vivo* experiments originate from the inhibitory effect of secreted OPN on the crystal growth of apatite *in vivo*, which competes with the induced activity of osteoblasts.

We thank Olympus Optical, Co., Ltd. for the β-TCP porous materials used as ceramic scaffolding in the experiments. We thank Mr. Yi Liu of Fudan Univ. (China) for his assistance in SEM observation.

REFERENCES

1. Giachelli, C.M., Schwartz, S.M., and Liaw, L.(1995) Molecular and cellular biology of osteopontin. *Trends Cardiovasc. Med.* **3**, 88–95
2. Rittling, S.R. and Denhardt, D.T. (1999) Osteopontin function in pathology: lessons from osteopontin-deficient mice. *Exp. Nephrol.* **7**, 103–113
3. Giachelli, C.M. and Steitz, S. (2000) Osteopontin: a versatile regulator of inflammation and biomineralization. *Matrix Biol.* **19**, 615–622
4. Murry, C.E., Giachelli, C.M., Schwartz, S.M., and Vracko, R.(1994) Macrophages express osteopontin during repair of myocardial necrosis. *Amer. J. Pathol.* **145**, 1450–1462
5. Liaw, L., Lindner, V., Schwartz, S.M., Chambers, A.F., and Giachelli, CM. (1995) Osteopontin and beta 3 integrin are coordinately expressed in regenerating endothelium in vivo and stimulate Arg-Gly-Asp–dependent endothelial migration *in vitro*. *Circ. Res.* **77**, 665–672
6. Scatena, M., Almeida, M., Chaisson, M.L., Fausto, N., Nicosia, R.F., and Giachelli, C.M. (1998) NF-kappaB mediates alphavbeta3 integrin–induced endothelial cell survival. *J. Cell Biol.* **141**, 1083–1093
7. Buttler, W.T., Ridall, A.L., and McKee, M.D. (1996) Osteopontin. in *Principles of Bone Biology* (Bilezikian, J.P., Raisz, L.G, . and Rodan, G.A., eds.) pp. 167–181, Academic Press, New York
8. Noda, M. and Denhardt, D.T.(2002) Osteopontin in *Principles of Bone Biology*, *2nd Ed.* (Bilezikian, J.P., Raisz, L.G., Rodan, G.A., eds.) pp. 239–250, Academic Press, New York
9. Butler, W.T. (1989) The nature and significance of osteopontin. *Connect. Tissue Res.* **23**, 123–136
10. Yabe, T., Nemoto, A., and Uemura, T. (1997) Recognition of osteopontin by rat bone marrow derived osteoblastic primary cells. *Biosci. Biotechnol. Biochem.* **61**, 754–756
11. Liu, Y-K., Uemura, T., Nemoto, A., Yabe, T., Fujii, N., Ushida, T., and Tateishi, T. (1997) Osteopontin involvement in integrin-mediated cell signaling and regulation of expression of alkaline phosphatase. *FEBS Lett.* **420**, 112–116
12. Mark, M.P., Butler, W.T., Prince, C.W., Finkelman, R.D., and Ruch, J.V. (1988) Developmental expression of 44-kDa bone phosphoprotein (osteopontin) and bone gamma-carboxyglutamic acid (Gla)–containing protein (osteocalcin) in calcifying tissues of rat. *Differentiation* **37**, 123–136
13. Reinholt, F.P., Hultenby, K., Oldberg, A., and Heinegard, D. (1990) Osteopontin–a possible anchor of osteoclasts to bone. *Proc. Natl Acad. Sci. USA.* **87**, 4473–4475
14. Ross, F.P., Chappel, J., Alvarez, J.I., Sander, D., Butler, W.T., Farach-Carson, M.C., Mintz, K.A., Robey, P.G., Teitelbaum, S.L., and Cheresh, D.A. (1993) Interactions between the bone matrix proteins osteopontin and bone sialoprotein and the osteoclast integrin alpha v beta 3 potentiate bone resorption. *J. Biol. Chem.* **268**, 9901–9907
15. Chellaiah, M. and Hruska, K. (1996) Osteopontin stimulates gelsolin-associated phosphoinositide levels and phosphatidylinositol triphosphate-hydroxyl kinase. *Mol. Biol. Cell.* **7**, 743–753
16. Chellaiah, M., Fitzgerald, C., Alvarez, U., and Hruska, K. (1998) c-Src is required for stimulation of gelsolin-associated phosphatidylinositol 3-kinase. *J. Biol. Chem.* **273**, 11908–11916
17. Chellaiah, M.A., Soga, N., Swanson, S., McAllister, S., Alvarez, U., Wang, D., Dowdy, S.F., and Hruska, K.A. (2000) Rho-A is critical for osteoclast podosome organization, motility, and bone resorption. *J. Biol. Chem.* **275**, 11993–12002
18. Uemura, T., Liu, Y-K., and Kuboki, Y. (2000) mRNA expression of MT1-MMP, MMP-9, cathepsin K, and TRAP in highly enriched osteoclasts cultured on several matrix proteins and ivory surfaces. *Biosci. Biotechnol. Biochem.* **64**, 1771–1773
19. Chellaiah, M., Kizer, N., Silva, M., and Alvarez, U. Kwiatkowski, D.K., Hrska, A. (2000) Gelsolin deficiency blocks podosome assembly and produces increased bone mass and strength. *J. Cell Biol.* **148**, 665–678
20. Suzuki, K., Zhu, B., Rittling, S.R., Denhardt, D.T., Goldberg, H.A., Mcculloch, C.A.G., and Sodek, J. (2002) Colocalization of intracellular osteopontin with CD44 is associated with migration, cell fusion and resorption in osteoclasts. *J. Bone Miner. Res.* **17**, 1486–1497
21. Boskey, A.L., Maresca, M., Ullrich, W., Doty, S.B., Butler, W.T., and Prince, C.W. (1993) Osteopontin-hydroxyapatite interactions *in vitro*: inhibition of hydroxyapatite formation and growth in a gelatin-gel. *Bone Miner.* **22**, 147–159
22. Hunter, G.K. and Goldberg, H.A. (1993) Nucleation of hydroxyapatite by bone sialoprotein. *Proc. Natl. Acad. Sc.i USA* **90**, 8562–8565
23. Hunter, G.K., Kylem C.L., and Goldberg, H.A. (1994) Modulation of crystal formation by bone phosphoproteins: structural specificity of the osteopontin-mediated inhibition of hydroxyapatite formation. *Biochem. J.* **300**, 723–728
24. Ihara, H., Denhardt, D.T., Furuya, K., Yamashita, T., Muguruma, Y., Tsuji, K., Hruska, K.A., Higashio, K., Enomoto, S., Nifuji, A., Rittling, S.R., and Noda, M. (2001) Parathyroid hormone–induced bone resorption does not occur in the absense of osteopontin. *J. Biol. Chem.* **276**, 13065–13071
25. Asou, Y., Rittling, S.R., Yoshitake, H., Tsuji, K., Shinomiya, K., Nifuji, A., Denhardt, D.T., and Noda, M. (2001) Osteopontin facilitates angiogenesis, accumulation of osteoclasts, and resorption in ectopic bone. *Endocrinology* **142**, 1325–1332
26. Maniatopoulos, C., Sodek, J., and Melchen, A.H. (1988) Bone formation *in vitro* by stromal cells obtained from bone marrow of young adult rats. *Cell Tissue Res.* **254**, 317–330
27. Dong, J., Uemura, T., Shirasaki, Y., and Tateishi, T. (2002) Promotion of bone formation using highly pure porous beta-TCP combined with bone marrow–derived osteoprogenitor cells. *Biomaterials* **23**, 4493–4502
28. Uemura, T., Dong, J., Wang, Y., Kojima, H., Saito, T., Iejima, D., Kikuchi, M., Tanaka, J., and Tateishi, T. (2003) Transplantation of cultured bone cells using combinations of scaffolds and culture techniques. *Biomaterials* **24**, 2277–2286
29. Majeska, R.J., Port, M., and Einhorn, T.A. (1993) Attachment to extracellular matrix molecules by cells differing in the expression of osteoblastic traits. *J. Bone Miner. Res.* **8**, 277–289.
30. Lee, Y.J., Park, S.J., Lee, W.K., Ko, J.S., and Kim, H.M. (2003) MG63 osteoblastic cell adhesion to the hydrophobic surface precoated with recombinant osteopontin fragments. *Biomaterials* **24**, 1059–1066
31. Katayama, Y., House, C.M., Udagawa, N., Kazama, J.J., McFarland, R.J., Martin, T.J., and Findlay, D.M. (1998) Casein kinase 2 phosphorylation of recombinant rat osteopontin enhances adhesion of osteoclasts but not osteoblasts. *J. Cell Physiol.* **176**, 179–187
32. Cheng, S.L., Lai, C.F., Blystone, S.D., and Avioli, L.V. (2001) Bone mineralization and osteoblast differentiation are negatively modulated by integrin alpha(v)beta3. *J Bone Miner. Res.* **16**, 277–288
33. Alden, T.D., Pittman, D.D., Beres, E.J., Hankins, G.R., Kallmes, D.F., Wisotsky, B.M., Kerns, K.M., and Helm, G.A. (1999) Percutaneous spinal fusion using bone morphogenetic protein-2 gene therapy. *J. Neurosurg.* **90 (Suppl. 1)**, 109–114
34. Baltzer, A.W., Lattermann, C., Whalen, J.D., Wooley, P., Weiss, K., Grimm, M., Ghivizzani, S.C., Robbins, P.D., and Evans, C.H. () Genetic enhancement of fracture repair: healing of an experimental segmental defect by adenoviral transfer of the BMP-2 gene. *Gene Ther.* **7**, 734–739
35. Franceschi, R.T., Wang, D., Krebsbach, P.H., and Rutherford, R.B. (2000) Gene therapy for bone formation: in vitro and in vivo osteogenic activity of an adenovirus expressing BMP7. *J. Cell. Biochem.* **678**, 476–486
36. Helm, G.A., Alden, T.D., Beres, E.J., Hudson, S.B., Das, S., Engh, J.A., Pittman, D.D., Kern, K.M., and Kallmes, D.F. (2000) Use of bone morphogenetic protein-9 gene therapy to induce spinal arthrodesis in the rodent. *J. Neurosurg* **92 (Suppl 2)**, 191–196

37. Musgrave, D.S., and Bosch, P. Ghivizzani, S., Robbins, P.D., Evans, C.H., and Huard, J. (1999) Adenovirus-mediated direct gene therapy with bone morphogenetic protein-2 produces bone. *Bone* **24**, 541–547
38. Flores, M.E., Norgard, M., Heinegard, D., Reinholt, F.P., and Andersson, G. (1992) RGD-directed attachment of isolated rat osteoclasts to osteopontin, bone sialoprotein, and fibronectin. *Exp. Cell Res.* **201**, 526–530
39. Ross, F.P., Chappel, J., Alvarez, J.I., Sander, D., Butler, W.T., Farach-Carson, M.C., Mintz, K.A., Robey, P.G, . Teitelbaum, S.L., and Cheresh, D.A. (1993) Interactions between the bone matrix proteins osteopontin and bone sialoprotein and the osteoclast integrin alpha v beta 3 potentiate bone resorption. *J. Biol. Chem.* **268**, 9901–9907